HHS Public Access

Author manuscript

Magn Reson Med. Author manuscript; available in PMC 2019 December 01.

Published in final edited form as:

Magn Reson Med. 2018 December ; 80(6): 2598–2608. doi:10.1002/mrm.27361.

Simultaneous T1 and T2 Mapping of the Carotid Plaque (SIMPLE) with T2 and Inversion Recovery Prepared 3D Radial Imaging

Haikun Qi[1], **Jie Sun**[2], **Huiyu Qiao**[1], **Xihai Zhao**[1], **Rui Guo**[1], **Niranjan Balu**[2], **Chun Yuan**[1,2], and **Huijun Chen**[1]

[1]Center for Biomedical Imaging Research, Department of Biomedical Engineering, School of Medicine, Tsinghua University, Beijing, China

[2]Department of Radiology, University of Washington, Seattle, Washington, USA

Abstract

Purpose—To propose a technique which can produce different T1 and T2 contrasts in a single scan for simultaneous T1 and T2 mapping of the carotid plaque (SIMPLE).

Methods—An interleaved 3D golden angle radial trajectory was used in conjunction with T2 preparation with variable duration (TE_{prep}) and inversion recovery pulses. Sliding window reconstruction was adopted to reconstruct images at different inversion delay time and TE_{prep} for joint T1 and T2 fitting. In the fitting procedure, a rapid B1 correction method was presented. The accuracy of SIMPLE was investigated in phantom experiments. In vivo scans were performed on five healthy volunteers with two scans each, and on five patients with carotid atherosclerosis.

Results—The phantom T1 and T2 estimations of SIMPLE agreed well with the standard methods with the percentage difference smaller than 7.1%. In vivo T1 and T2 for normal carotid vessel wall were 1213±48.3ms and 51.1±1.7ms, with good inter-scan repeatability. Alternations of T1 and T2 in plaque regions were in agreement with the conventional multi-contrast imaging findings.

Conclusion—The proposed SIMPLE allows simultaneous T1 and T2 mapping of the carotid artery in less than 10min, serving as a quantitative tool with good accuracy and reproducibility for plaque characterization.

Keywords

carotid artery; atherosclerosis; 3D radial; T1 mapping; T2 mapping

INTRODUCTION

Carotid atherosclerosis is a leading cause of ischemic stroke (1,2). Histopathological studies have suggested that, similar to coronary atherosclerosis, plaque composition plays an essential role in clinical complications associated with carotid atherosclerosis (3,4). Consequently, there have been tremendous efforts to develop noninvasive imaging methods

Correspondence to: Huijun Chen, Rm109, Center for Biomedical Imaging Research, School of Medicine, Tsinghua University, Haidian District, Beijing, 100084, China, Tel No: +86-10-62798332, chenhj_cbir@mail.tsinghua.edu.cn.

for in vivo characterization of high-risk carotid plaque, such as those with large lipid-rich necrotic core (LRNC) and/or intraplaque hemorrhage (IPH) (5). As different plaque components have different T1 and/or T2 relaxation times, MRI has emerged as the most promising imaging modality for accurate quantification of carotid plaque components (3,6). A multi-contrast MR imaging protocol including time-of-flight (TOF), T1-weighted (T1w) and T2-weighted (T2w) turbo spin echo (TSE) sequences is typically used, in which each component displays a unique combination of hyper- or hypo-intense signals on the multi-contrast images (7,8). However, given its qualitative nature, multi-contrast MRI suffers relatively high variability in measuring plaque components because of numerous factors that may affect relative signal intensities, such as subjective reader interpretation, coil positioning, and imaging parameters (9–12). Moreover, multi-contrast imaging requires long scan time (> 15 min) and complex registration of different contrasts, which may limit its clinical application. Fast quantitative T1 and T2 mapping of carotid plaque technique can resolve the above problems by facilitating voxel-by-voxel classification of plaque components. Eliminating the need for signal intensity normalization and thus improving the reproducibility of tissue characterization by carotid MRI, T1 and T2 mapping techniques may find wide application in longitudinal or multi-center studies.

A few recent studies have explored in vivo T1 or T2 mapping of the carotid artery (13–17). Biasiolli et al. quantified T2 relaxation times of different plaque components by using a 2D multi-echo spin echo sequence (13). By utilizing 3D black-blood preparation of variable preparation times, Yuan et al. proposed a 3D T2 mapping sequence with larger coverage and thinner slices (16). By utilizing inversion recovery (IR) prepared 3D golden angle radial sampling, Qi et al. developed a 3D T1 mapping technique (GOAL-SNAP) with large coverage and isotropic spatial resolution (15). Coolen et al. were the first to develop a combined 3D vessel wall T1 and T2 mapping technique (14). Nonetheless, at least four separate scans were needed, which resulted in relatively long scan duration and may incur errors due to image mis-registration and B1 inhomogeneity. Besides, with only two data points in T1 or T2 mapping, T1 and T2 fitting can be vulnerable to noise (14).

In this work, we present a technique that allows simultaneous T1 and T2 mapping of carotid plaque (SIMPLE) with large coverage and 3D isotropic resolution in an 8-minute scan. It utilizes variable duration T2 preparation and inversion recovery (T2IR) for generating different T1 and T2 contrasts and 3D golden angle radial acquisition for efficient sampling (18). Since the center of k-space is repeatedly sampled by each radial spoke, the T2IR signal curve is finely sampled. By using view sharing and sliding window reconstruction, a set of coregistered 3D high resolution images with different T1 and T2 contrasts is generated, which subsequently yields quantitative T1 and T2 maps. Phantom and volunteer scans were performed to evaluate the accuracy and repeatability of T1 and T2 mapping by SIMPLE. Patients with carotid atherosclerosis were also imaged, in which T1 and T2 maps of carotid plaques by SIMPLE were compared with conventional multi-contrast images.

METHODS

Sequence Design

As shown in the sequence diagram (Fig. 1a), SIMPLE acquisition is prepared with both adiabatic T2 preparation (19) and IR pulses (T2IR) to generate T1 and T2 contrasts. To induce different T2 weightings, the duration of T2 preparation (TE_{prep}) is varied in each turbo field echo (TFE) shot. When TE_{prep} is set to zero, the T2 preparation module is not performed in that TFE shot (20,21), which is then only IR prepared. After a short time (T_{gap}), a series of RF pulses with a small flip angle (θ) are performed as is in a standard spoiled gradient echo sequence. For fat suppression, spatial–spectral pulse for selective water excitation is adopted. Before the next T2IR, there is an amount of time (T_{ex}) to allow the longitudinal magnetization to recover.

Following T2IR preparation, 3D radial sampling is adopted for 3D isotropic acquisition. The 3D golden angle radial order proposed for the GOAL-SNAP sequence (15) is modified for SIMPLE to achieve an uniform distribution of spokes used for reconstruction at a certain TI and TE_{prep}. Specifically, spokes acquired at the same TI in the shots with the same TE_{prep} (S1, S1′, Fig1a), conform to the golden angle distribution, with the azimuthal angle and polar angle increments ($\Delta\tau$ and $\Delta\upsilon$) defined by the 2D golden angle means ϕ_1=0.4656, ϕ_2=0.6823 (18):

$$\Delta\upsilon(\mathrm{S1},\mathrm{S1}') = a\cos\left(\phi_1\right),\quad \Delta\tau(S1,S1') = 2\pi\cdot\phi_2 \qquad [1]$$

while for adjacent spokes in one shot (S1, S2, Fig. 1a), the azimuthal angle and polar angle increments are defined by:

$$\Delta\upsilon(S1,S2) = a\cos\left(\left\{M/mTE\cdot\phi_1\right\}\right),\quad \Delta\tau(S1,S2) = 2\pi\cdot\left\{M/mTE\cdot\phi_2\right\} \qquad [2]$$

where {} means getting the fraction parts, M is the total number of shots, mTE is the number of different T2IR durations. For spokes of the same TI in adjacent shots (S1, S3, Fig. 1a), the corresponding angle increments are defined as follows:

$$\Delta\upsilon(\mathrm{S1},\ \mathrm{S3}) = a\cos\left(\left\{M/mTE\cdot N\cdot\phi_1\right\}\right),\quad \Delta\tau(\mathrm{S1},\ \mathrm{S3}) = 2\pi\cdot\left\{M/mTE\cdot N\cdot\phi_2\right\} \qquad [2]$$

where N is the TFE factor.

Signal acquired by each spoke can be obtained by simulations according to the sequence parameters. The longitudinal magnetization for the first θ pulse, $M_\theta(1)$ is:

$$M_\theta(1) = M_0 - \left(M_0 + \alpha\cdot M_{before\_T2IR}\cdot E_2\right)E_{gap} \qquad [4]$$

where M_0 is the fully relaxed longitudinal magnetization, M_{before_T2IR} is the longitudinal magnetization before T2IR, $E_2 = \exp(-TE_{prep}/T_2)$, $E_{gap} = \exp(-T_{gap}/T_1)$, and α is the inversion efficiency of the IR pulse. Then, the longitudinal magnetization right before the kth (k>1) θ pulse, $M_\theta(k)$, is:

$$M_\theta(k) = M_\theta(1)\left(E_1 cos\theta\right)^{k-1} + M_0\left(1 - E_1\right)\frac{1 - \left(E_1 cos\theta\right)^{k-1}}{1 - E_1 cos\theta} \quad [5]$$

where E_1 is defined as $E_1 = \exp(-TR/T_1)$, and TR is the time of repetition of the θ pulse. Lastly, the longitudinal magnetization before the next T2IR is:

$$M_z\left(T_{ex}\right) = M_\theta(N+1)E_e + M_0\left(1 - E_e\right) \quad [6]$$

where E_e is defined as $E_e = \exp(-T_{ex}/T_1)$.

Ignoring T_2* decay, the longitudinal magnetization can be assumed to be the measured signal. Then, based on Eq. [4-6], signals acquired by each spoke can be determined. After several repetitions of TFE shots with alternate TE_{prep}, the steady-state signal will be achieved. The illustrative steady-state signal curves are shown in Fig. 1b.

Image Reconstruction and T1/T2 Fitting

For image reconstruction, to increase the signal-to-noise ratio (SNR), the sliding window reconstruction is performed by combining all spokes with spoke number from n to $n + TW - 1$ in all shots with the same TE_{prep}. TW is the temporal window width, and n is from 1 to $N - TW + 1$, with an interval of TW. To reduce undersampling artifacts, the iterative conjugate gradient (CG) SENSE reconstruction is applied (22). Coil sensitivity maps are estimated by using spokes at TI larger than 1300ms instead of all data to reduce phase errors associated with the inverted longitudinal magnetization. Additionally, the sensitivity maps are reconstructed in low resolution by using only the central half of k-space data to reduce noise. The low resolution sensitivity maps are also used to correct phase errors in inverted signals.

Since the image contrast is dominated by k-space center, the image intensity of the sliding window reconstruction is determined by averaging the signals of projections from n to $n + TW - 1$, which is defined in Eq. [5]. By fitting the signal curve from the reconstructed image series to the theoretically simulated signal, T1, T2 and α can be estimated voxel-by-voxel. Considering that variations of the θ pulse caused by B1 inhomogeneity may influence T1 and T2 estimation. The scaling parameter μ between the actual flip angle and the nominal flip angle should also be fitted with $\theta = \mu\theta_{norm}$, and θ_{norm} is the nominal flip angle. To account for the additional unknown μ and α, the T2IR data are combined with separately acquired spoiled gradient echo (SPGR) data at two or more flip angles for fitting. And the unique solution for M_0, T_1, T_2, α and μ can be determined by the least squares minimization of the object function combining T2IR and SPGR data:

$$f(M_0,\ T_1,\ T_2,\ \alpha,\ \mu) = \sum_n \left[M_n - S_{T2IR,n}\right]^2 + \sum_{i=1}^{N_\beta} \left[\frac{M_0(1-E_1)sin(\mu\beta_i)}{1-E_1 cos(\mu\beta_i)} - S_{SPGR,i}\right]^2 \quad [7]$$

where $S_{T2IR,n}$ is the signal of the n^{th} reconstructed frame of the T2IR data, M_n is the corresponding simulated signal, and the index n runs through all T2IR images; N_β is the number of SPGR images, $S_{SPGR,i}$ is the measured signal intensity of SPGR images at the nominal flip angle β_i. The combined fitting with SPGR images for simultaneous T1, inversion efficiency and B1 estimation has been successfully applied in previous studies of brain T1 mapping (23,24).

Based on a priori knowledge that inversion efficiency and B1 field maps should be smooth, a two-step procedure is used in T1 and T2 fitting. Firstly, all the five parameters ($M_0,\ T_1,\ T_2,\ \alpha,\ \mu$) are fitted by the least squares minimization of Eq. [7]. The resulting α and μ maps are smoothed by a median filter and then used as known values in the second fitting for the other three parameters ($M_0,\ T_1,\ T_2$). The object function of the second fitting only includes T2IR data:

$$f(M_0,\ T_1,\ T_2) = \sum_n \left[M_n - S_{T2IR,n}\right]^2 \quad [8]$$

Using the α and μ as a priori information reduces the number of degrees of freedom and has been shown to improve the accuracy and precision in the fitting for T1 and T2 (24). The coefficient of determination is used to determine fitting quality. And T1 and T2 values of pixels with coefficient of determination <0.95 are set to zero.

Carotid Imaging Protocol

The proposed sequence was designed for carotid imaging. All imaging experiments were performed on a 3.0T Philips MR scanner (Achieva TX, Best, The Netherlands). The imaging parameters are shown in Table 1. Three alternate TE_{prep} of 0, 25, 50ms were adopted in SIMPLE, resulting in an 8-minute scan. Immediately following SIMPLE acquisition, two SPGR images (45 seconds each) were acquired using 3D radial trajectory with nominal flip angles different from that of SIMPLE. To reduce undersampling artifacts, the SPGR images were also reconstructed with CG-SENSE iteration. Low resolution sensitivity maps were estimated directly from the SPGR radial data by using only the central half data. For image reconstruction, TW of sliding window was selected to be 25 (250ms/frame), resulting in 21 frames. T1/T2 estimation was performed voxel-by-voxel by using the above mentioned two-pass fitting procedure.

For carotid wall depiction, similar to the GOAL-SNAP work (15), a black-blood image with near-zero luminal signal (Fig. 1b) was reconstructed using KWIC technique to achieve both

high spatial resolution and high SNR (25). The black-blood image was used to delineate vessel wall boundaries, referred to as SIMPLE vessel wall (VW) image hereafter.

Phantom Experiments

Phantom scans were performed on 12 tubes with different T1 and T2 values, which were made of different concentrations of agarose (Sigma-Aldrich, Saint Louis, USA) and Gd-DTPA (Magnevist, Bayer Pharma AG, Germany). The diameter of the tubes is 1.5cm, and they are fixed on a tube holder for imaging with the distance between adjacent tube centers to be 2.1cm. Quantitative T1 and T2 mapping of the phantoms were performed using SIMPLE as well as standard 2D T1 and T2 mapping sequences: IR-spin echo (IR-SE) and multi-echo spin echo (ME-SE). Only the center slice of the SIMPLE image was imaged by the 2D mapping techniques. The imaging parameters of the 2D IR-SE were: FOV=140×108mm^2, spatial resolution=1.6×1.7mm^2, slice thickness=5mm, TR/TE=15000/8.7ms, 14 inversion times = [100, 200, 300, 400, 500, 600, 700, 800, 900, 1000, 1500, 2000, 2500, 3000]ms. The 2D ME-SE was performed with the same geometry setting to the 2D IR-SE, and other parameters included: TR=15000ms, 8 TE values ranging from 8.5ms to 68ms with an interval of 8.5ms. The imaging parameters of SIMPLE were the same to the in vivo imaging. The scan time of SIMPLE was 8 minutes, and the scan duration of 2D IR-SE and ME-SE were 3 hours 44 minutes and 16.5 minutes, respectively.

In vivo Experiments

Five healthy volunteers (3 males; 25.4±2.3 years) and five patients (5 males; 64.2±5.2 years) with carotid atherosclerosis were recruited in this study. The healthy volunteers were imaged twice on two separate days to test the repeatability of vessel wall T1/T2 measurements. Informed consent was obtained from all subjects, and this study was approved by the institutional review board. All subjects were imaged using a commercially available 8-channel carotid coil (Chenguang, Shanghai, China). Besides SIMPLE, healthy volunteers were also imaged by 2D MOLLI (26) and 2D T2prep-bSSFP (27) techniques with FOV=160×160mm^2, spatial resolution=1.5×1.5mm^2, 1 slice, slice thickness=5mm. The MOLLI and T2prep-bSSFP were performed with low spatial resolution to maintain the SNR for accurate T1 and T2 estimation, and they were used as references for muscle measurements. Patients were also imaged by conventional 2D multi-contrast sequences including TOF, black-blood T1w-TSE and T2w-TSE (8) and SNAP sequence (28).

Image Analysis

SIMPLE and SPGR images were reconstructed as described above for T1 and T2 estimation. For phantom images by SIMPLE and 2D IR-SE and ME-SE, circular regions of interest (ROI) were drawn on each tube and the mean T1, T2 values and standard deviation (SD) were calculated for each tube. And to view the measurement variability of SIMPLE in each tube, the histograms of T1 and T2 were also plotted for each tube. For healthy volunteer data, SIMPLE image data were reformatted into slices that matched the scan plane of MOLLI and T2prep-bSSFP. ROIs with area of about 28mm^2 were drawn on the sternocleidomastoid muscle on both sides. The mean and standard deviation (SD) of T1 and T2 values of muscle were recorded. To assess reproducibility of vessel wall T1 and T2 measurements, SIMPLE images were reformatted into 0.8 mm axial slices, and the in-plane

spatial resolution of the reformatted images was interpolated to $0.4\times0.4mm^2$. Three nonadjacent slices of the common carotid artery (CCA) below the carotid bifurcation were analyzed for carotid arteries on both sides. Lumen and outer wall boundaries were drawn on the SIMPLE VW image using an in-house software developed in MATLAB R2016b (MathWorks, Natick, Massachusetts, USA). The mean T1 and T2 values of carotid vessel wall were calculated for each slice. And then the average and SD of the mean values from all slices were reported for healthy vessel wall. The selected slices for T1 and T2 measurements were matched between repeated scans by using carotid bifurcation as the landmark. For atherosclerotic arteries, reformatted axial slices with thickness of 0.8mm and in-plane spatial resolution of $0.4\times0.4mm^2$ centered at the plaque were analyzed. And the estimated T1 and T2 maps were compared with conventional multi-contrast and SNAP images.

Statistical Analysis

Phantom T1 and T2 measurements by SIMPLE were compared with 2D IR-SE and ME-SE using the Pearson's correlation and Bland-Altman analyses. In vivo T1 and T2 values of muscle estimated by SIMPLE were compared with MOLLI and T2prep-bSSFP using the Wilcoxon rank-sum test. For the repeated scans, the first and second T1 or T2 measurements of muscle and vessel wall on matched axial slices were compared using the Wilcoxon rank-sum test and the Bland-Altman analysis. And the inter-scan coefficient of variation (CV) was also calculated (29). Furthermore, to account for dependence among slices from the same artery, vessel wall measurements were compared using a permutation test based on the Wilcoxon rank-sum test, where data was permutated by artery. And for vessel wall CV calculation, the bootstrap and percentile method was used to calculate the 95% confidence interval (CI), where resampling was performed by artery. All statistics were performed using SPSS (Version 19.0, SPSS Inc). $P<0.05$ was considered statistically significant.

RESULTS

Phantom Study

The T1 and T2 maps of phantoms by SIMPLE were similar to those by the spin echo references as shown in Figure 2. The mean T1 and T2 values by SIMPLE were in good agreement with those by 2D IR-SE and ME-SE (T1: $R^2=0.99$; T2: $R^2=0.99$; Figure 3a). Bland-Altman plots showed no apparent relationship between the difference and average of T1 or T2 measurements by SIMPLE and 2D IR-SE, ME-SE (T1: $P=0.09$; T2: $P=0.08$, Fig. 3b). The histograms of T1 and T2 values estimated by SIMPLE in each tube were provided and compared with the 2D spin echo methods in the Supporting file. Compared to 2D IR-SE, 2D ME-SE, the percent errors of T1 estimation by SIMPLE is ranging from 0.64% to 4.2%, and of T2 is from 0.07% to 7.1%. And the mean and SD of percent errors were 2.2% ±1.2 and 2.8%±1.9 for SIMPLE T1 and T2 measurements, respectively.

In vivo Study

All 10 subjects successfully completed the study. Figure 4 shows representative images in a healthy volunteer. Vessel wall is clearly seen on the reconstructed black-blood image (Fig. 4b). The T1 and T2 maps by SIMPLE were similar to those by MOLLI and T2prep-bSSFP (Fig. 4b and 4c). The T1 and T2 of muscle estimated by SIMPLE and MOLLI, T2prep-

bSSFP were compared and no significant differences were noted: T1, 1027±32.3ms vs. 1012±22.1ms, P=0.22; T2, 30.3±1.1ms vs. 31.8±2.1ms, P=0.12. For repeated scans of muscle, no significant differences were observed between the two measurements of MOLLI (T1: P=0.88), T2prep-bSSFP (T2: P=0.97) and SIMPLE (T1: P=0.82; T2: P=0.85). The CV values were 0.81%, 1.0% for muscle T1 by MOLLI and SIMPLE, and 1.0%, 1.1% for muscle T2 by T2prep-bSSFP and SIMPLE. There were also no significant differences between the first and second T1 or T2 measurements of carotid vessel wall by SIMPLE (n=30; T1: 1213±48.3ms vs. 1221±52.3ms, P=0.52; T2: 51.1±1.7ms vs. 51.9±2.1ms, P=0.19). And the inter-scan CVs of vessel wall measurements were 2.7% (95% CI: 1.9%, 3.5%) and 4.8% (95% CI: 3.8%, 5.6%) for T1 and T2, respectively.

Eight carotid plaques were identified in the five patients. IPH was detected on SNAP images in five plaques. Figure 5 shows two representative slices of a carotid plaque with IPH, which shows hyperintensity on SNAP image and isointensity on T2w image. T1 mapping indicates T1 is substantially reduced in the IPH region. Figure 6 shows another plaque with IPH and calcification (hypointensity on all contrasts). A portion of the IPH region has hyperintense signals on T2w image. While T1 mapping again shows reduced T1, T2 mapping indicates variable T2 in the IPH region with higher T2 in the regions corresponding to hyperintensities on T2w image. Pixels in calcification regions had low SNR and low coefficient of determination (<0.95), so the T1 and T2 were set to zero. The images of one plaque without IPH, which had lipid, loose matrix and calcification identified on multi-contrast images (6) are shown in Fig. 7. T1 and T2 mapping results show low T2 values of lipid, and elevated T1 and T2 values in the loose matrix region. And the T1 and T2 values of calcification in this plaque were set to be zero.

DISCUSSION

A technique for simultaneous T1 and T2 mapping of vessel wall was developed in this study. The proposed sequence adopted both T2 and IR preparations to facilitate acquisition of different T1 and T2 contrasts, followed by 3D golden angle radial sampling for time-efficient acquisition. Sliding window reconstruction then generated a series of T1 and T2 contrasts for quantitative mapping. A rapid B1 correction method was adopted in the T1/T2 fitting procedure to correct B1 inhomogeneity. The accuracy of T1 and T2 mapping by SIMPLE was demonstrated in the phantom study. Moreover, the in vivo study in healthy volunteers and patients with carotid atherosclerosis showed the feasibility and great potential of SIMPLE for quantitative atherosclerosis imaging.

Recently, there has been increasing interest in quantitative mapping of atherosclerosis for more automated and reproducible measurements of plaque composition. In vivo T2 mapping of plaque has been shown to be able to quantify lipid-rich core in carotid atherosclerosis (13,17). On the other hand, T1 mapping may be the preferred way to monitor the IPH progression (15,30,31), which is a key risk factor for clinical events. To fulfill these needs, this study proposed the SIMPLE sequence for simultaneous plaque T1 and T2 quantification in a single 3D large coverage scan with the advantage of relative short scan time and good accuracy.

The in vivo quantifications of atherosclerotic plaque by SIMPLE revealed the clear alternations of T1 and/or T2 in the plaque region, which were in agreement with signal intensity changes on the conventional multi-contrast images. For example, in T1 maps, the regions with reduce T1 values corresponded to the regions with hyperintensity on SNAP (Fig.5, 6). In T2 maps, the regions with elevated T2 values showed high signal on T2w-TSE (Fig. 6, 7), while the regions with low T2 had low signal on T2w-TSE (Fig. 7). As for IPH evaluation, all the imaged IPH regions showed decreased T1 values estimated by SIMPLE, which reflected previous finding (15). But the elevated T2 values were only observed in one plaque with IPH (Fig. 6), which may be associated with recent IPH (32). So with the ability of simultaneous T1 and T2 quantification, SIMPLE may provide complementary histological information of IPH. Lipid-rich necrotic core is another important plaque component in carotid atherosclerosis. A recent study with histological validation revealed that T2 mapping can characterize the LRNC in carotid plaque (17). And the ability of SIMPLE to quantify lipid core was demonstrated by the T2 mapping of a lipid plaque, which displays low signal on T2w images (Fig. 7).

Technically, radial sampling was used in SIMPLE, which is intrinsically less sensitive to motion than Cartesian sampling (33), and has been used in free breathing abdominal imaging (34). So radial acquisition enables the SIMPLE image reconstruction without motion artifacts corruption. Besides, the adopted 3D golden angle radial sampling is also the key technique for efficient acquisition and flexible reconstruction. Combing the T2IR preparation with 3D golden radial acquisition, SIMPLE is able to generate a series of images with different contrasts for T1 and T2 fitting. In this study, the temporal window width to reconstruct one T2IR frame is 250ms, with a total of 21 frames of T2IR series, the time interval between the first frame and the last frame is about 6 seconds. And the inter-frame motion in the short time can be negligible, so there is no need of registration of the T2IR images before fitting. Considering that B1 inhomogeneity will introduce bias to the excitation and preparation pulses, which may influence the accuracy of T1 and T2 estimation, so in the T1 and T2 fitting procedure, a rapid B1 calibration method was presented. This method combined the T2IR images with SPGR images acquired at different flip angles to correct for B1 inhomogeneity. Similar methods were used in previous studies of T1 mapping (23,24). The high accuracy and reproducibility found in phantom and in vivo studies further indicate the feasibility of the proposed method.

According to previous studies of vessel wall T1 mapping (14,15), the T1 value of carotid plaque should be in the range of 200-1500ms. For T2, Biasiolli, et al., has reported the T2 values of vessel wall (54ms), lipid rich necrotic core (37ms), fibrous tissue (56ms) and recent IPH (107ms) (13). And it can be seen that except for the recent IPH, most T2 values of carotid plaque are in the range of 35 to 55ms. In this study, the imaging parameters of SIMPLE, such as the inversion recovery time of 2000ms and T2prep duration of 0, 25 and 50ms, were set for carotid plaque with moderate T1 and T2 values. But the estimation accuracy of larger T1 and T2 values is not expected to be as good as the smaller T1 and T2. As the phantom results shown, lower accuracy and higher variation were observed for larger T1 and T2 values estimated by SIMPLE. This is because after IR pulse, the magnetization recovery of larger T1 was slower than that of smaller T1, so the SNR of the tubes with larger T1 was lower than smaller T1. And then the larger T1 values were estimated with larger

variations. For T2 estimation accuracy, the major influence is the duration of T2prep, TE_{prep}. The largest TE_{prep} is usually set similar to the T2 value to be estimated (20,21). If the largest TE_{prep} is too small, the range of T2 decay curve will be too small, and if it is too large, the SNR of the signal after T2 decay will be too low, both of which will influence the accuracy of T2 estimation. In this study, TE_{prep} values of 0, 25ms and 50ms were chosen to cover most T2 values of carotid plaque. But the TE_{prep} values may not be optimal for larger T2, the measurement variation of which will be increased due to the reduced T2 decay range. Therefore, for future studies, if targeted at large T1, the amount of samples across the recovery curve should be increased. And for larger T2, the duration of T2prep should be increased to improve the estimation accuracy.

To reduce the undersampling artifacts, 250ms view sharing was adopted in T2IR image series reconstruction. The choice of temporal window width of view sharing is a tradeoff between the reconstructed SNR and the dynamic range for fitting. View sharing will increase the signal of the first point at the magnetization recovery curve, and thus reduce the dynamic range of magnetization, especially for short T1, which experiences faster recovery. While in one previous study of brain T1 mapping (24), they've demonstrated 300ms view sharing can still produce accurate estimation for T1 less than 200ms. Similarly, in our study, temporal window width of 250ms also had good estimation accuracy (0.8% difference compared with 2D IR-SE) for T1 of 326ms. The current reconstruction setting has shown to be feasible for carotid artery imaging, and further optimization of the sliding window width was not covered in this study.

The 8-minutes scan time of SIMPLE was tolerated well by all the volunteers and patients in this study, and no motion artifacts were observed in the image reconstructed from radial data. However, for wider application of SIMPLE, its performance can be further improved by using advanced reconstruction algorithms such as compressed sensing and low-rank (35,36), which can be used to shorten the scan time, improve the reconstructed image quality, or increase the spatial resolution of SIMPLE. Besides, although 0.8mm isotropic spatial resolution was used in previous study of 3D vessel wall imaging (37) and 0.7mm isotropic spatial resolution was used in in previous study of 3D carotid artery T1 and T2 mapping (14), we agree the 0.7mm or the 0.8mm spatial resolution used in this study, may be suboptimal to image thin vessel wall. However, these techniques including SIMPLE sequence, are not aimed at normal thin vessel wall, but proposed for imaging of carotid plaque, which is featured with thickened vessel wall (focal wall thickness > 2mm), so the 0.8mm spatial resolution was chosen considering its tradeoff with SNR and acquisition time.

There are several limitations in this study. Firstly, although utilizing phase-sensitive inversion recovery reconstruction method, a black-blood image can be reconstructed from SIMPLE to delineate lumen and vessel wall, as a common issue in IR-based techniques for carotid artery imaging (28,38), the possible recirculated blood flow at the carotid bifurcation or blood flow with very fast or slow velocity may cause flow artifacts in SIMPLE VW. And the flow artifacts may influence the measurements of SIMPLE in the juxta-luminal region. Secondly, we lacked histology validation for the in vivo experiments due to the unavailability of histological specimens. However, the conventional multi-contrast imaging which has been histologically validated in previous studies was used as reference for plaque

characterization (8). Furthermore, more patients should be recruited in future studies to further investigate the proposed sequence.

CONCLUSIONS

This study developed a fast high spatial resolution technique for simultaneous 3D T1 and T2 mapping of vessel wall, which showed excellent agreement in measuring T1 and T2 of phantoms with traditional 2D spin echo methods and high reproducibility in preliminary studies of healthy volunteers. Compared with existing T1-weighted and T2-weighted techniques, SIMPLE may allow us to obtain more quantitative and reproducible measurements of atherosclerotic plaque.

Supplementary Material

Refer to Web version on PubMed Central for supplementary material.

References

1. Takaya N, Yuan C, Chu BC, Saam T, Underhill H, Cai JM, Tran N, Polissar NL, Isaac C, Ferguson MS, Garden GA, Cramer SC, Maravilla KR, Hashimoto B, Hatsukami TS. Association between carotid plaque characteristics and subsequent ischemic cerebrovascular events - A prospective assessment with MRI - Initial results. Stroke. 2006; 37(3):818–823. [PubMed: 16469957]
2. Gupta A, Baradaran H, Schweitzer AD, Kamel H, Pandya A, Delgado D, Dunning A, Mushlin AI, Sanelli PC. Carotid Plaque MRI and Stroke Risk A Systematic Review and Meta-analysis. Stroke. 2013; 44(11):3071–3077. [PubMed: 23988640]
3. Trivedi RA, U-King-Im J, Graves MJ, Horsley J, Goddard M, Kirkpatrick PJ, Gillard JH. Multi-sequence in vivo MRI can quantify fibrous cap and lipid core components in human carotid atherosclerotic plaques. Eur J Vasc Endovasc. 2004; 28(2):207–213.
4. Redgrave JNE, Lovett JK, Gallagher PJ, Rothwell PM. Histological assessment of 526 symptomatic carotid plaques in relation to the nature and timing of ischemic symptoms - The Oxford plaque study. Circulation. 2006; 113(19):2320–2328. [PubMed: 16651471]
5. Saam T, Hatsukami TS, Takaya N, Chu BC, Underhill H, Kerwin WS, Cai JM, Ferguson MS, Yuan C. The vulnerable, or high-risk, atherosclerotic plaque: Noninvasive MR imaging for characterization and assessment. Radiology. 2007; 244(1):64–77. [PubMed: 17581895]
6. Saam T, Ferguson MS, Yarnykh VL, Takaya N, Xu D, Polissar NL, Hatsukami TS, Yuan C. Quantitative evaluation of carotid plaque composition by in vivo MRI. Arteriosclerosis, thrombosis, and vascular biology. 2005; 25(1):234–239.
7. Fayad ZA, Fuster V. Clinical imaging of the high-risk or vulnerable atherosclerotic plaque. Circ Res. 2001; 89(4):305–316. [PubMed: 11509446]
8. Cai JM, Hastukami TS, Ferguson MS, Small R, Polissar NL, Yuan C. Classification of human carotid atherosclerotic lesions with in vivo multicontrast magnetic resonance imaging. Circulation. 2002; 106(11):1368–1373. [PubMed: 12221054]
9. Li FY, Yarnykh VL, Hatsukami TS, Chu BC, Balu N, Wang JN, Underhill HR, Zhao XH, Smith R, Yuan C. Scan-Rescan Reproducibility of Carotid Atherosclerotic Plaque Morphology and Tissue Composition Measurements Using Multicontrast MRI at 3T. J Magn Reson Imaging. 2010; 31(1): 168–176. [PubMed: 20027584]
10. Touze E, Toussaint JF, Coste J, Schmitt E, Bonneville F, Vandermarcq P, Gauvrit JY, Douvrin F, Meder JF, Mas JL, Oppenheim C, Grp HS. Reproducibility of high-resolution MRI for the identification and the quantification of carotid atherosclerotic plaque components consequences for prognosis studies and therapeutic trials. Stroke. 2007; 38(6):1812–1819. [PubMed: 17463311]

11. Wasserman BA, Astor BC, Sharrett AR, Swingen C, Catellier D. MRI Measurements of Carotid Plaque in the Atherosclerosis Risk in Communities (ARIC) Study: Methods, Reliability and Descriptive Statistics. J Magn Reson Imaging. 2010; 31(2):406–415. [PubMed: 20099354]
12. Sun J, Zhao XQ, Balu N, Hippe DS, Hatsukami TS, Isquith DA, Yamada K, Neradilek MB, Canton G, Xue YJ, Fleg JL, Desvigne-Nickens P, Klimas MT, Padley RJ, Vassileva MT, Wyman BT, Yuan C. Carotid magnetic resonance imaging for monitoring atherosclerotic plaque progression: a multicenter reproducibility study. Int J Cardiovas Imag. 2015; 31(1):95–103.
13. Biasiolli L, Lindsay AC, Chai JT, Choudhury RP, Robson MD. In-vivo quantitative T2 mapping of carotid arteries in atherosclerotic patients: segmentation and T2 measurement of plaque components. J Cardiovasc Magn Reson. 2013; 15:69. [PubMed: 23953780]
14. Coolen BF, Poot DH, Liem MI, Smits LP, Gao S, Kotek G, Klein S, Nederveen AJ. Three-dimensional quantitative T1 and T2 mapping of the carotid artery: Sequence design and in vivo feasibility. Magn Reson Med. 2016; 75(3):1008–1017. [PubMed: 25920036]
15. Qi H, Sun J, Qiao H, Chen S, Zhou Z, Pan X, Wang Y, Zhao X, Li R, Yuan C, Chen H. Carotid Intraplaque Hemorrhage Imaging with Quantitative Vessel Wall T1 Mapping: Technical Development and Initial Experience. Radiology. 2017
16. Yuan J, Usman A, Reid SA, King KF, Patterson AJ, Gillard JH, Graves MJ. Three-dimensional black-blood T2 mapping with compressed sensing and data-driven parallel imaging in the carotid artery. Magn Reson Imaging. 2017; 37:62–69. [PubMed: 27888153]
17. Chai JT, Biasiolli L, Li LQ, Alkhalil M, Galassi F, Darby C, Halliday AW, Hands L, Magee T, Perkins J, Sideso E, Handa A, Jezzard P, Robson MD, Choudhury RP. Quantification of Lipid-Rich Core in Carotid Atherosclerosis Using Magnetic Resonance T-2 Mapping Relation to Clinical Presentation. Jacc-Cardiovasc Imag. 2017; 10(7):747–756.
18. Chan RW, Ramsay EA, Cunningham CH, Plewes DB. Temporal Stability of Adaptive 3D Radial MRI Using Multidimensional Golden Means. Magn Reson Med. 2009; 61(2):354–363. [PubMed: 19165897]
19. Nezafat R, Stuber M, Ouwerkerk R, Gharib AM, Desai MY, Pettigrew RI. B1-insensitive T2 preparation for improved coronary magnetic resonance angiography at 3 T. Magn Reson Med. 2006; 55(4):858–864. [PubMed: 16538606]
20. Blume U, Lockie T, Stehning C, Sinclair S, Uribe S, Razavi R, Schaeffter T. Interleaved T-1 and T-2 Relaxation Time Mapping for Cardiac Applications. J Magn Reson Imaging. 2009; 29(2):480–487. [PubMed: 19161206]
21. Giri S, Chung YC, Merchant A, Mihai G, Rajagopalan S, Raman SV, Simonetti OP. T2 quantification for improved detection of myocardial edema. J Cardiovasc Magn R. 2009; 11
22. Pruessmann KP, Weiger M, Bornert P, Boesiger P. Advances in sensitivity encoding with arbitrary k-space trajectories. Magn Reson Med. 2001; 46(4):638–651. [PubMed: 11590639]
23. Deoni SC. High-resolution T1 mapping of the brain at 3T with driven equilibrium single pulse observation of T1 with high-speed incorporation of RF field inhomogeneities (DESPOT1-HIFI). J Magn Reson Imaging. 2007; 26(4):1106–1111. [PubMed: 17896356]
24. Kecskemeti S, Samsonov A, Hurley SA, Dean DC, Field A, Alexander AL. MPnRAGE: A technique to simultaneously acquire hundreds of differently contrasted MPRAGE images with applications to quantitative T1 mapping. Magn Reson Med. 2016; 75(3):1040–1053. [PubMed: 25885265]
25. Song HK, Dougherty L. k-space weighted image contrast (KWIC) for contrast manipulation in projection reconstruction MRI. Magn Reson Med. 2000; 44(6):825–832. [PubMed: 11108618]
26. Messroghli DR, Radjenovic A, Kozerke S, Higgins DM, Sivananthan MU, Ridgway JP. Modified Look-Locker inversion recovery (MOLLI) for high-resolution T1 mapping of the heart. Magn Reson Med. 2004; 52(1):141–146. [PubMed: 15236377]
27. Giri S, Chung YC, Merchant A, Mihai G, Rajagopalan S, Raman SV, Simonetti OP. T2 quantification for improved detection of myocardial edema. Journal of cardiovascular magnetic resonance : official journal of the Society for Cardiovascular Magnetic Resonance. 2009; 11:56. [PubMed: 20042111]
28. Wang JN, Bornert P, Zhao HL, Hippe DS, Zhao XH, Balu N, Ferguson MS, Hatsukami TS, Xu JR, Yuan C, Kerwin WS. Simultaneous noncontrast angiography and intraPlaque hemorrhage (SNAP)

imaging for carotid atherosclerotic disease evaluation. Magn Reson Med. 2013; 69(2):337–345. [PubMed: 22442116]

29. Bland JM, Altman DG. Measurement error. Brit Med J. 1996; 312(7047):1654–1654. [PubMed: 8664723]
30. van den Bouwhuijsen QJA, Selwaness M, Tang H, Niessen WJ, Hofman A, Franco OH, van der Lugt A, Vernooij MW. Change in Carotid Intraplaque Hemorrhage in Community-dwelling Subjects: A Follow-up Study Using Serial MR Imaging. Radiology. 2017; 282(2):526–533. [PubMed: 27541684]
31. Wang X, Sun J, Zhao X, Hippe DS, Hatsukami TS, Liu J, Li R, Canton G, Song Y, Yuan C. Ipsilateral plaques display higher T1 signals than contralateral plaques in recently symptomatic patients with bilateral carotid intraplaque hemorrhage. Atherosclerosis. 2017; 257:78–85. [PubMed: 28110259]
32. Chu BC, Kampschulte A, Ferguson MS, Kerwin WS, Yarnykh VL, O'Brien KD, Polissar NL, Hatsukami TS, Yuan C. Hemorrhage in the atherosclerotic carotid plaque: A high-resolution MRI study. Stroke. 2004; 35(5):1079–1084. [PubMed: 15060318]
33. Glover GH, Pauly JM. Projection Reconstruction Techniques for Reduction of Motion Effects in Mri. Magn Reson Med. 1992; 28(2):275–289. [PubMed: 1461126]
34. Feng L, Grimm R, Block KT, Chandarana H, Kim S, Xu J, Axel L, Sodickson DK, Otazo R. Golden-Angle Radial Sparse Parallel MRI: Combination of Compressed Sensing, Parallel Imaging, and Golden-Angle Radial Sampling for Fast and Flexible Dynamic Volumetric MRI. Magn Reson Med. 2014; 72(3):707–717. [PubMed: 24142845]
35. Doneva M, Bornert P, Eggers H, Stehning C, Senegas J, Mertins A. Compressed sensing reconstruction for magnetic resonance parameter mapping. Magn Reson Med. 2010; 64(4):1114–1120. [PubMed: 20564599]
36. Zhao B, Lu W, Hitchens TK, Lam F, Ho C, Liang ZP. Accelerated MR parameter mapping with low-rank and sparsity constraints. Magn Reson Med. 2015; 74(2):489–498. [PubMed: 25163720]
37. Zhou ZC, Li R, Zhao XH, He L, Wang XL, Wang JN, Balu N, Yuan C. Evaluation of 3D multi-contrast joint intra- and extracranial vessel wall cardiovascular magnetic resonance. J Cardiov Magn Reson. 2015; 17
38. Wang JN, Ferguson MS, Balu N, Yuan C, Hatsukami TS, Bornert P. Improved Carotid Intraplaque Hemorrhage Imaging Using a Slab-Selective Phase-Sensitive Inversion-Recovery (SPI) Sequence. Magn Reson Med. 2010; 64(5):1332–1340. [PubMed: 20597120]

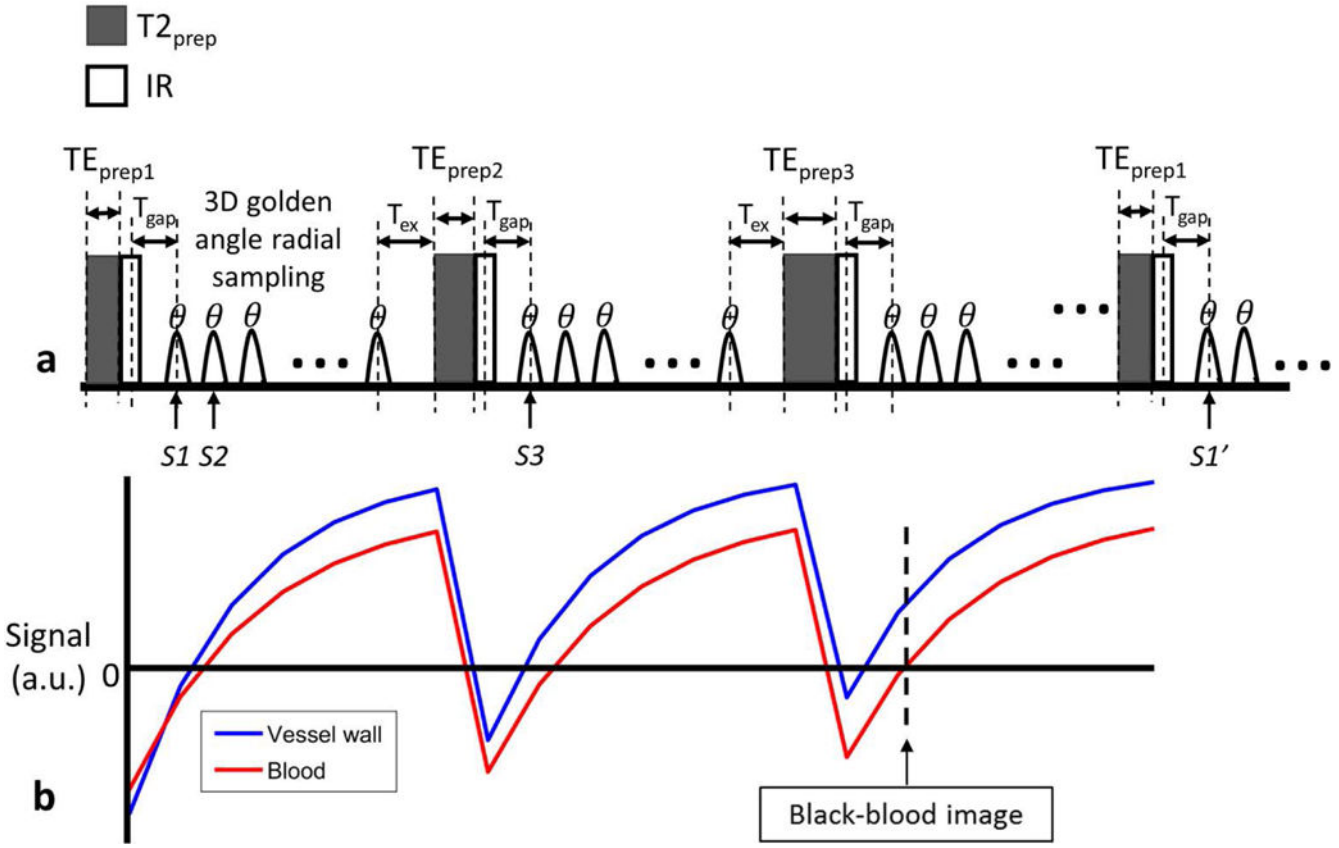

FIG.1.

a: The schematic diagram of the T2 and IR prepared 3D golden angle radial sequence, where the three shown sequence blocks have different duration of T2 preparation. After preparation, spoiled gradient echoes were acquired with flip angle of θ. T_{gap} is the time between the IR pulse and the first gradient echo, and T_{ex} is the time between the last gradient echo acquisition and the next T2 preparation. S1 and S2 indicate the two adjacent spokes in one shot; S1 and S1′ indicate the two spokes acquired at the same TI in two nearest shots with the same TE_{prep}; S1 and S3 indicate the two spokes acquired at the same TI in two adjacent shots. **b**: The simulated T2IR signal evolutions of vessel wall and blood. And the black-blood vessel wall image is reconstructed at the near zero point of blood.

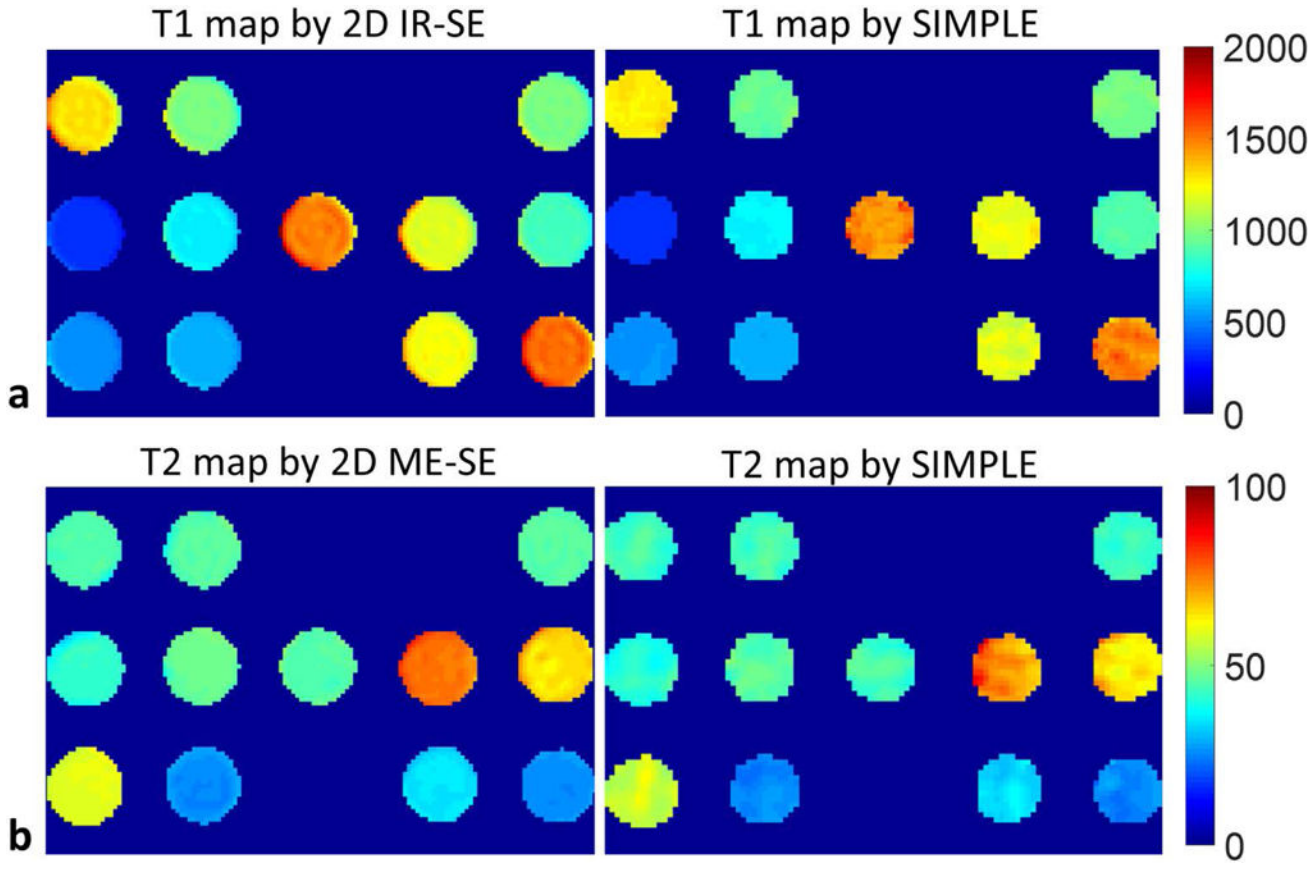

FIG. 2.

a: The T1 maps of phantom estimated by 2D IR-SE and SIMPLE. **b**: The T2 maps of phantom estimated by 2D ME-SE and SIMPLE.

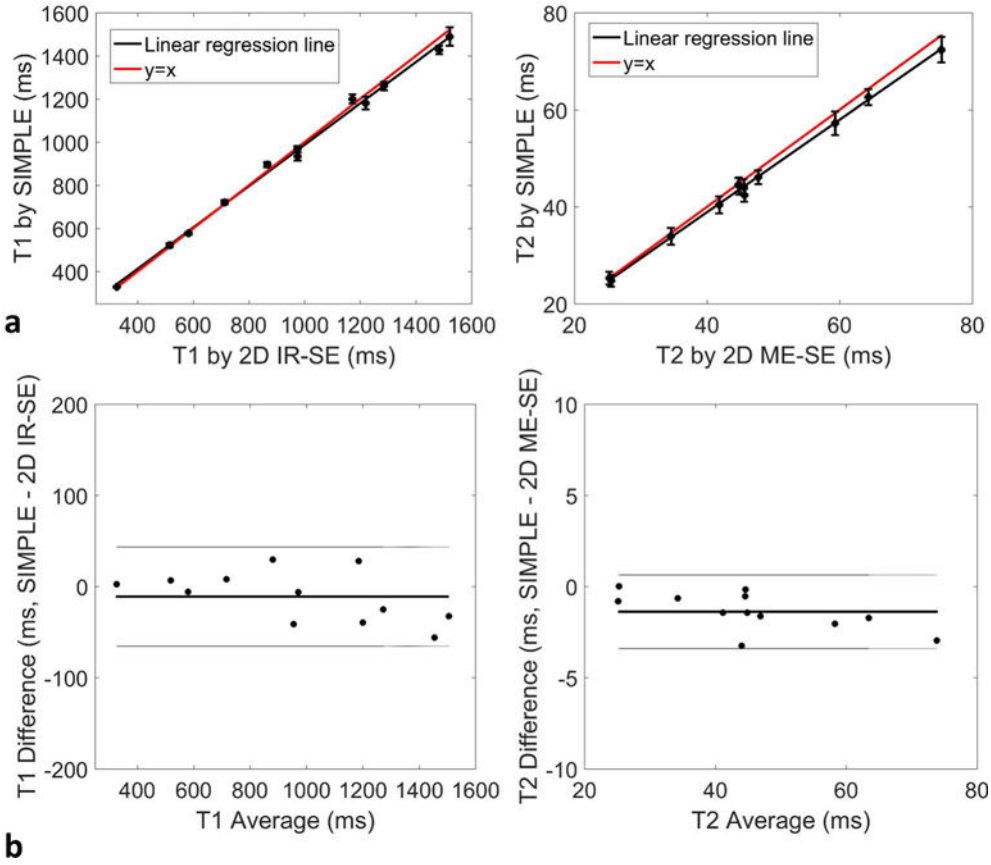

FIG. 3.

a: Comparison of T1 and T2 measurements of phantoms between SIMPLE and 2D standard spin echo methods with mean and SD shown. The black line indicates the linear regression line, and the red line represents y=x. **b**: Bland-Altman plot showing the difference between the two methods with the mean value. The solid line indicates the average difference, and the dotted lines indicate the 95% confidence intervals for T1 and T2.

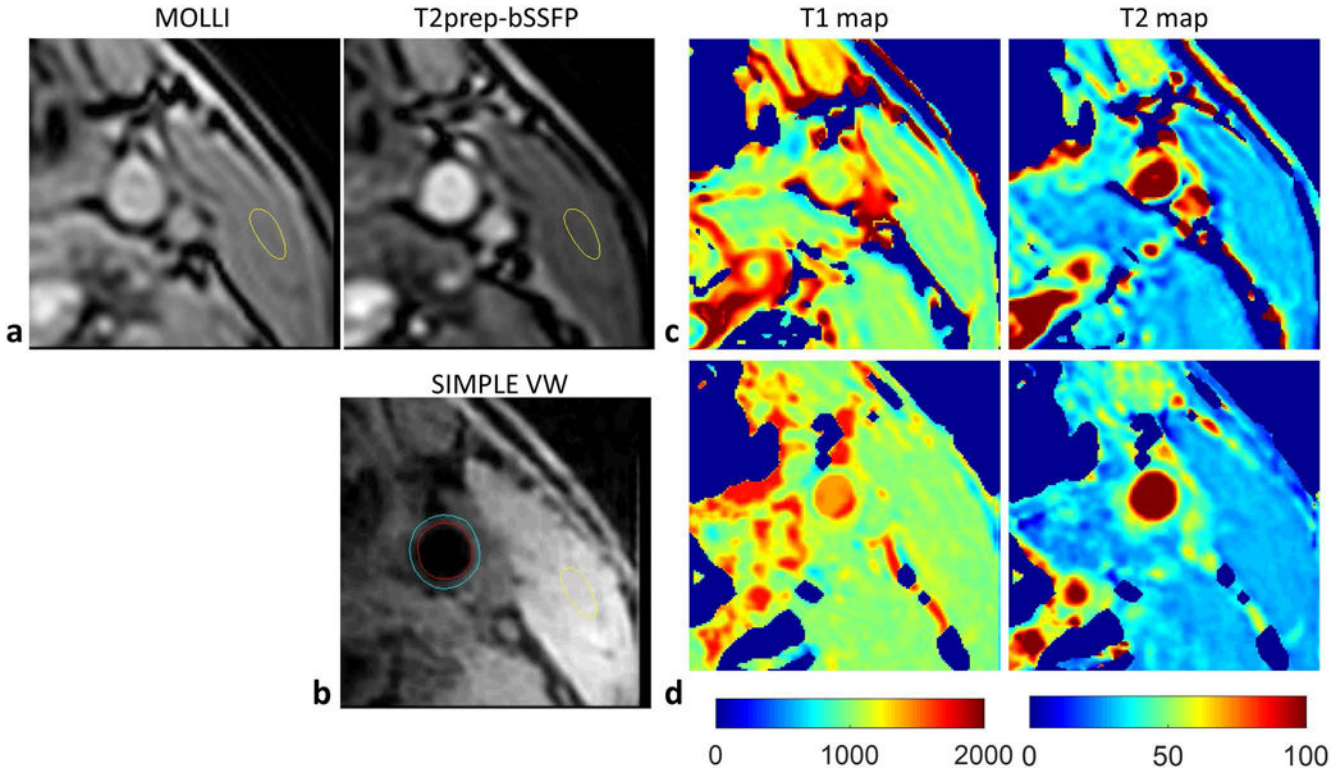

FIG. 4.

Carotid artery T1 and T2 mapping of a healthy volunteer. **a**, **b**: The MOLLI, T2prep-bSSFP images, and the black-blood vessel wall images reconstructed from SIMPLE. The yellow contour indicates the ROI of muscle, and the blue and red contour indicates the ROI of outer wall and lumen. **c**: The T1 and T2 maps measured using MOLLI and T2prep-bSSFP methods. **d**: The T1 and T2 maps estimated by SIMPLE.

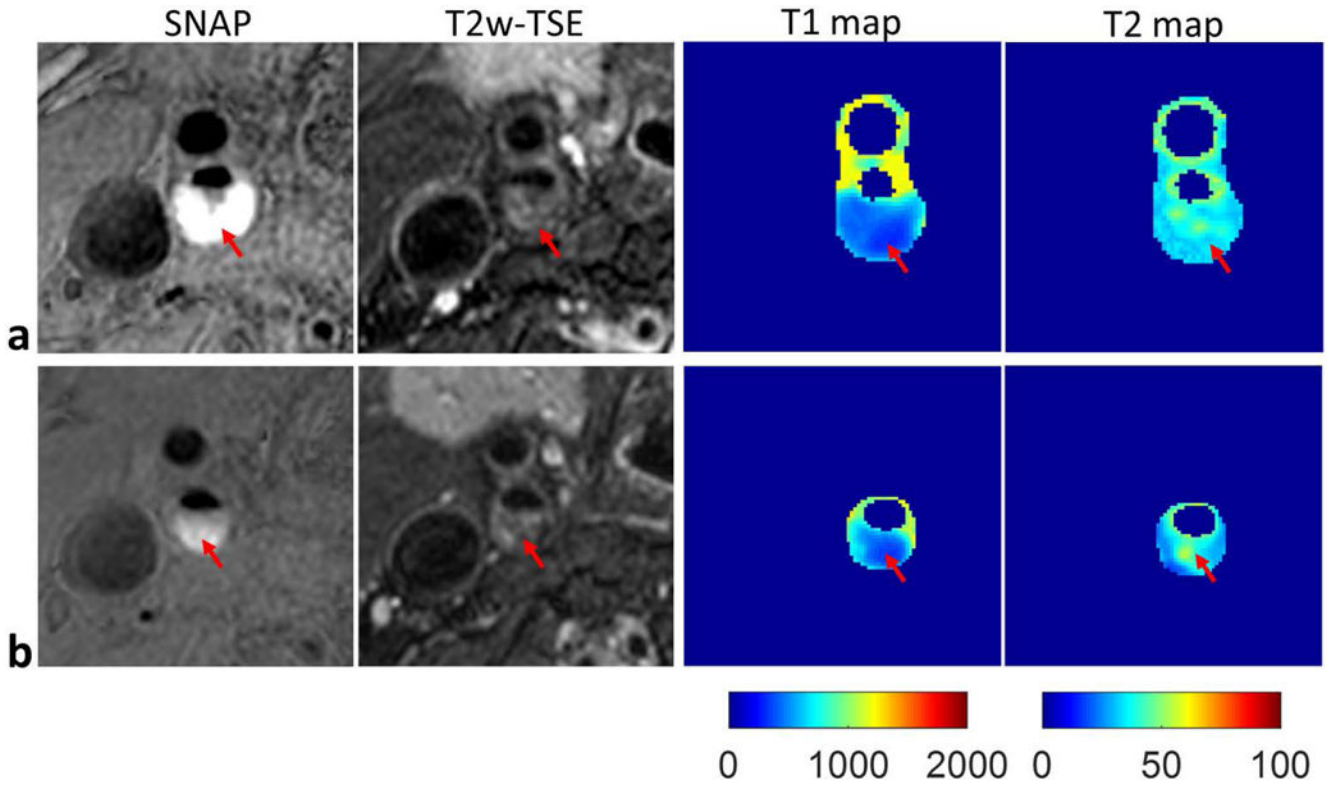

FIG. 5.

Carotid artery T1 and T2 mapping of an atherosclerotic plaque (male, 61 years old) by SIMPLE. Two representative slices were shown (**a**, **b**), including the SNAP, T2w-TSE images and the T1, T2 maps estimated by SIMPLE. The red arrow indicates the IPH region. Lower T1 values and no obvious alterations of T2 values were found in the IPH, which were in agreement with the SNAP and T2w-TSE images, respectively.

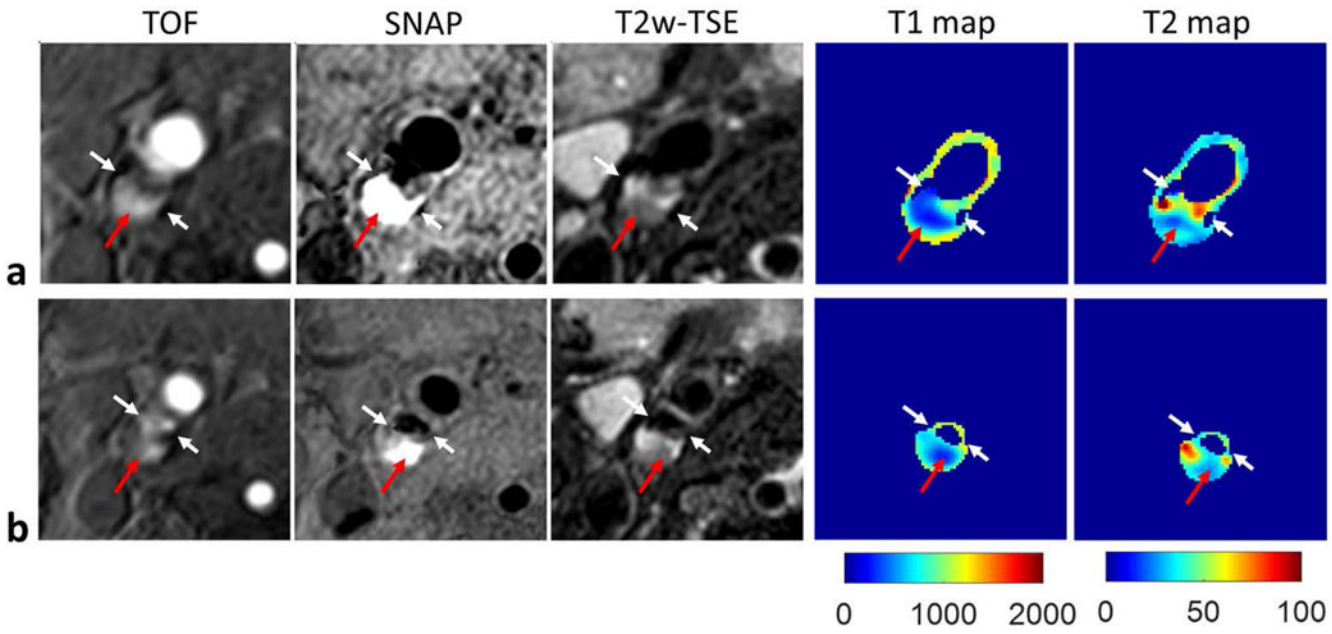

FIG. 6.

T1 and T2 mapping of one carotid plaque (male, 72 years old) with both IPH and calcification by SIMPLE. The TOF, SNAP and T2w-TSE images, and the T1, T2 maps generated by SIMPLE from two slices of the plaque are shown in **a**, **b**, separately. The white arrows indicate the calcification, and the red arrows indicate the IPH region. Compared with surrounding region, lower T1 values were observed in the IPH region, while higher T2 values were only observed in a portion of IPH. The T1 and T2 of calcification cannot be reliably fitted, and were set to be zero.

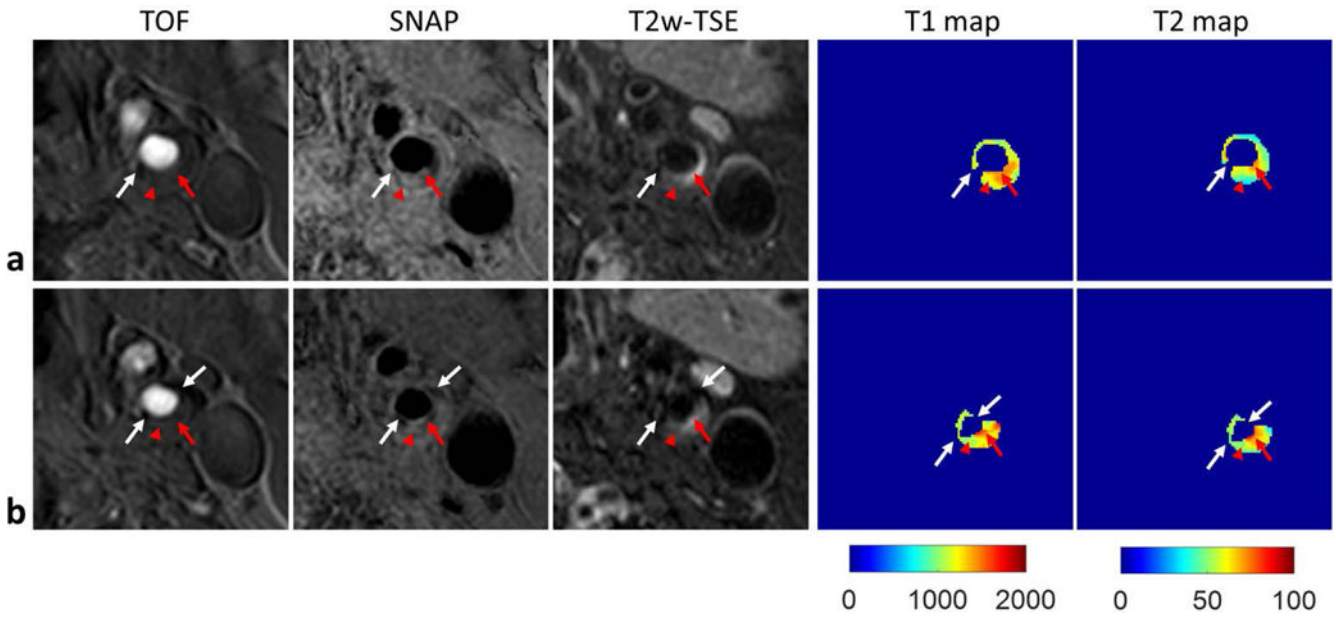

FIG. 7.

Carotid artery T1 and T2 mapping of a plaque (male, 60 years old) featured with lipid, loose matrix and calcification by SIMPLE. Two central slices of the plaque are shown in **a**, **b**, including the TOF, SNAP and T2w-TSE images, and the T1, T2 maps estimated from SIMPLE. The red arrow heads indicate the lipid where low T2w signal and low T2 values were observed, and the red arrows indicate the loose matrix region with high signal on T2w image and low signal on T1w image, where elevated T1 and T2 values were found. The white arrows indicate the calcification, where the T1 and T2 cannot be reliably fitted, and were set to be zero.

Table 1

Imaging parameters of SIMPLE and 3D radial SPGR scan

	FOV (mm^3)	Voxel Size (mm)	TR/TE (ms)	Flip angle	TFE factor (N)	T_{gap} (ms)	T_{ex} (ms)	Scan duration
SIMPLE	120×120×120	0.8 isotropic	10/4.0	8°	175	10 [b]	250	8min
SPGR	120×120×120	1 isotropic	10/4.0	6°/10° [a]	NA	NA	NA	45s

[a] The SPGR images were acquired with 2 nominal flip angles of 6° and 10°

[b] The minimum values allowed on the scanner

NA: not applicable